

**SOMATOSENSORY BRAIN RESPONSES EVOKED BY
VIBROTACTILE STIMULATION OF THE DISTAL
PHALANX IN NORMAL SUBJECTS**

by

DUYGU TORUN

B.S. Systems Engineering, Yeditepe University Engineering& Architecture Faculty,
2006

Submitted to the Institute of Biomedical Engineering
in partial fulfillment of the requirements
for the degree of
Master of Science
in
Biomedical Engineering

Boğaziçi University

June 2009

ACKNOWLEDGMENTS

Firstly, I would like to thank Assoc. Prof. Burak GÜÇLÜ for his advises and his guidance for my thesis and my life.

Many thanks also to Deniz NEVŞEHİRLİ and Mustafa Zahid YILDIZ for helping me in the lab.

My thanks also go to all my friends who never left me alone when I was in trouble with many problems

Special thanks to Duygu TORUN for her extra-ordinary friendship.

Thanks to my parents for financial and psychological supports.

And finally never enough thanks to Dr. Aeron Daniel PRESS for his brotherhood.

ABSTRACT

SOMATOSENSORY BRAIN RESPONSES EVOKED BY VIBROTACTILE STIMULATION OF THE DISTAL PHALANX IN NORMAL SUBJECTS

The sensory response upon vibrotactile stimuli is still not completely understood. Previously, the responses of single units from mechanoreceptive afferents and cortical neurons have been studied. On the other hand, there is a thorough psychophysical literature on judgements of the presence, magnitude, and frequency of vibrotactile stimuli. However, non-invasive recording of evoked somatosensory brain responses on the scalp was not explored adequately due to technical difficulties. Dependency of the evoked somatosensory response to vibrotactile stimuli, the frequency following response, is a phenomenon in which the human brain has a tendency to change its dominant EEG frequency towards the frequency of the external stimulus. This may arise from the synchronous firing of many cortical neurons. In this study, 40 and 230 Hz vibrotactile stimuli were applied to 10 adult subjects (5 females and 5 males) and psychophysical detection thresholds were measured at various frequencies using the two-interval forced choice paradigm. The psychophysical results were consistent with the literature. To measure the frequency following brain responses, stimulus amplitudes were determined based on the psychophysical sensation levels. Stimuli amplitudes were set at 10, 20 and 30 dB higher than the thresholds (SL=10, SL=20 and SL=30 dB respectively). EEG recordings were obtained over the primary somatosensory cortex with gold surface electrodes placed on the scalp at CPi-CPc. The results were examined by fourier transforms and wavelet transforms. Wavelet transform plots showed that, as the mechanical stimulus amplitude was increased, the background activity was suppressed and the frequency-following activity during the stimulus period increased. This finding was statistically significant. The origin of the frequency-following responses were discussed based on current results.

Keywords: taction, somatosensory cortex, mechanoreceptor, wavelet transform.

ÖZET

PARMAK UCUNUN MEKANİK TİTRESİMLE UYARILMASINA KARŞI BEYİNDEN OLCULEN FREKANS UYUMLU CEVAPLAR

Titreşimsel mekanik uyarılara karşı verilen duyuşsal cevaplar, halen tamamen anlaşılamamaktadır. Önceki çalışmalarda, mekanoreseptif aferentlerden ve kortikal nöronlardan tekil hücre cevapları araştırılmıştır. Öte yandan titreşimsel dokunma duyuşu uyarılarının varlığı, büyüklüğü ve frekansı ile ilgili derinlemesine yapılmış psikofiziksel çalışmalar da vardır . Ancak, kafatası üzerinden girişimsel olmayan uyarılmış potansiyeller ölçümü, teknik zorluklardan ötürü mekanik uyarılar kullanılarak yeterli olarak incelenmemiştir. Uyarılmış cevapların titreşimsel mekanik uyarılara bağlı olma durumu, yani frekans takipli cevaplar, insan beyninin kendi baskın EEG frekanslarını dışarıdan gelen uyarıların frekansına göre değiştirme eğiliminin gözüktüğü olgudur. Bu durum, birden fazla kortikal nöronun eş zamanlı ateşlenmesi ile açıklanabilir. Bu çalışmada, 5'i erkek 5'i kadın 10 yetişkine 40 ve 230 Hz frekanslarda mekanik titreşim uyarıları verilmiştir ve psikofiziksel eşik değerleri çift aralıklı zorlanmış seçenek yöntemi ile belirlenmiştir. Sonuçlar mevcut literatür ile tutarlı olarak bulunmuştur. Frekans takipli beyin cevaplarını ölçmek için kullanılan uyarı genlikleri psikofiziksel duyu seviyeleri temel alınarak belirlenmiştir. Verilen uyarıların seviyeleri duyu eşik değerlerinden 10(SL=10), 20(SL=20) ve 30(SL=30) dB daha yüksektir. EEG kayıtları be-denduyusu korteks bölgesi üzerinde, kafatası derisindeki CPi(+) ve CPc(-) noktalarına yerleştirilen altın elektrotlarla alınmıştır. Elde edilen sonuçlar, Fourier dönüşümü ve dalgacık dönüşümü ile incelenmiştir. Dalgacık dönüşümü grafiklerinden görüldüğü üzere, mekanik uyarı şiddeti arttıkça, beyin geriplan aktivitesi baskılanır ve uyarı süresince frekans takipli aktivite artar. Bu sonuçlar istatistiksel olarak anlamlı bulunmuştur. Frekans takipli cevapların kaynağı elde edilen yeni sonuçlar ile açıklanmıştır.

Anahtar Sözcükler:

TABLE OF CONTENTS

| | |
|---|------|
| ACKNOWLEDGMENTS | iii |
| ABSTRACT | iv |
| ÖZET | v |
| LIST OF FIGURES | viii |
| LIST OF TABLES | xi |
| LIST OF SYMBOLS | xii |
| LIST OF ABBREVIATIONS | xiii |
| 1. INTRODUCTION | 1 |
| 2. BACKGROUND | 2 |
| 2.1 Definition of the Psychophysics and Related Theory of Touch | 2 |
| 2.2 Somatosensory Evoked Potentials (SEPs) | 3 |
| 2.3 Anatomy of Skin and Mechanoreceptors | 5 |
| 2.3.1 Vibration Sense and Mechanoreceptors | 7 |
| 2.3.2 Mechano-electric transduction | 7 |
| 2.4 Primary Afferent Axons | 8 |
| 2.5 Dorsal Column-Medial Lemniscal Pathway | 9 |
| 2.6 Somatosensory Cortex | 12 |
| 2.6.1 Primary Somatosensory Cortex | 13 |
| 2.7 Frequency Following Responses | 14 |
| 3. METHOD | 15 |
| 3.1 Subjects | 15 |
| 3.2 Experimental Setup | 15 |
| 3.2.1 Apparatus | 15 |
| 3.2.2 Stimuli | 16 |
| 3.3 Experimental Protocol | 16 |
| 3.3.1 Part I | 17 |
| 3.3.2 Part II | 17 |
| 3.4 Analysis | 18 |
| 3.5 Wavelet Transform | 18 |

| | |
|---|----|
| 4. RESULTS | 21 |
| 4.1 Psychophysical Thresholds | 21 |
| 4.2 Somatosensory Evoked Potentials | 21 |
| 5. DISCUSSION | 27 |
| 6. CONCLUSION | 29 |
| 7. Limitations of the Study | 30 |
| 8. Future Work | 31 |
| APPENDIX A. APPENDIX A | 32 |
| APPENDIX B. APPENDIX B | 35 |
| APPENDIX C. APPENDIX C | 38 |
| REFERENCES | 42 |

LIST OF FIGURES

| | | |
|-------------|---|----|
| Figure 2.1 | Four channel model of mechanoreception with extended frequency ranges of the tuning curves [8]. | 3 |
| Figure 2.2 | Somatosensory evoked potentials to arm stimulation [9] | 4 |
| Figure 2.3 | Mechanoreceptors in the glabrous skin and the structure of their receptive field.[15] | 6 |
| Figure 2.4 | Variation among somatic sensory receptors of the skin in receptive field size and adaptation rate.[1] | 6 |
| Figure 2.5 | A rapidly adapting mechanoreceptor responds to sinusoidal mechanical stimuli with a single action potential for each cycle [15]. | 7 |
| Figure 2.6 | Frequency sensitivity of two fastly adapting tactile receptors of the skin [15]. | 7 |
| Figure 2.7 | Pacinian Corpuscle schematic diagram illustrated with its components [12] | 8 |
| Figure 2.8 | Structure of a segment of the spinal cord and its root. [1] | 9 |
| Figure 2.9 | Sensory information from limbs and trunk [15] | 10 |
| Figure 2.10 | The functional and anatomical organization of sensory processing networks .[15] | 11 |
| Figure 2.11 | Somatic sensory areas of the cortex. [1] | 12 |
| Figure 2.12 | Input pathway of sensory cortex from primarily one type of receptor. [15] | 13 |
| Figure 3.1 | Stimulus timing diagram for the two-interval forced-choice task | 16 |
| Figure 3.2 | Heisenberg Boxes; Time-frequency diagram of the wavelet transform. Representation of the window width which have simultaneous resolution in the time and frequency in wavelet transform [24]. | 19 |
| Figure 4.1 | Psychophysical thresholds. | 21 |
| Figure 4.2 | Somatosensory Evoked Potentials recorded from 1 subject. | 22 |
| Figure 4.3 | Psychophysical thresholds. | 22 |
| Figure 4.4 | Psychophysical thresholds. | 22 |

| | | |
|-------------|---|----|
| Figure 4.5 | Frequency following response recorded from SI of one subject evoked by mechanical vibrations at 40 Hz frequency and (A) 10 dB SL (B) 20 dB SL (C) 30 dB SL amplitude. | 23 |
| Figure 4.6 | Psychophysical thresholds. | 23 |
| Figure 4.7 | Psychophysical thresholds. | 23 |
| Figure 4.8 | Frequency following response recorded from SI of one subject evoked by mechanical vibrations at 230 Hz frequency and (A) 10 dB SL (B) 20 dB SL (C) 30 dB SL amplitude | 24 |
| Figure 4.9 | Psychophysical thresholds. | 24 |
| Figure 4.10 | Psychophysical thresholds. | 24 |
| Figure 4.11 | 19 Frequency following response recorded from SI of one subject evoked by mechanical vibrations at 40 Hz frequency and (A) 10 dB SL (B) 20 dB SL (C) 30 dB SL amplitude. (A) averaged for 8 subjects, (B)averages for 6 subjects and (C) averages for 5 subjects. | 25 |
| Figure 4.12 | Psychophysical thresholds. | 25 |
| Figure 4.13 | Psychophysical thresholds. | 25 |
| Figure 4.14 | 19 Frequency following response recorded from SI of one subject evoked by mechanical vibrations at 40 Hz frequency and (A) 10 dB SL (B) 20 dB SL (C) 30 dB SL amplitude. (A) averaged for 8 subjects, (B)averages for 6 subjects and (C) averages for 5 subjects. | 26 |
| Figure 5.1 | Control recordings for the 40 Hz evoked potentials. Left column: evoked potentials raw data, right column: power spectrum density. Red and blue lines represents control channel and CPi-CPc respectively. | 28 |
| Figure 5.2 | Control recordings for the 230 Hz evoked potentials. Left column: evoked potentials raw data, right column: power spectrum density while the stimulus were applying. Red and blue lines represents control channel and CPi-CPc respectively. | 28 |
| Figure A.1 | | 33 |
| Figure A.2 | | 33 |

| | |
|------------|----|
| Figure A.3 | 33 |
| Figure A.4 | 34 |
| Figure A.5 | 34 |
| Figure A.6 | 34 |
| Figure B.1 | 36 |
| Figure B.2 | 36 |
| Figure B.3 | 36 |
| Figure B.4 | 37 |
| Figure B.5 | 37 |
| Figure B.6 | 37 |
| Figure C.1 | 39 |
| Figure C.2 | 39 |
| Figure C.3 | 39 |
| Figure C.4 | 40 |
| Figure C.5 | 40 |
| Figure C.6 | 40 |
| Figure C.7 | 41 |
| Figure C.8 | 41 |

LIST OF TABLES

LIST OF SYMBOLS

| | |
|----------|-------------------------|
| a_{ij} | Description of a_{ij} |
| α | Description of α |

LIST OF ABBREVIATIONS

| | |
|-----|----------------------|
| LED | Light Emitting Diode |
| s | Second |
| FPS | Frame Per Second |
| A | Ampere |
| W | Watt |
| B | Magnetic Field |

1. INTRODUCTION

Somatic sensory system enables the human body to feel, ache, chill and know what its parts are performing. It is sensitive to numerous kinds of stimuli such as pressure and temperature. These are analyzed through the perception of touch, pain and temperature. The perception of touch begins at the skin. There are two major types of skin called hairy and glabrous (hairless) skin which have specialized receptors that convert mechanical stimulation into neural signals[1]. In the glabrous there are four kinds of mechanoreceptors; Pacinian corpuscles (Sato 1961), Merkel's disks (Munger 1979), Ruffini endings (Chambers 1972) and Meissner's corpuscles (Lindblom 1965) [2]. These receptors are sensitive to the physical distortions like bending or stretching and vary in their preferential stimulus frequencies, pressure, and receptive field sizes. Psychophysical and electrophysiological techniques have been frequently used to analyze tactile perception. Clinical experiments, on the other hand, were generally performed by using an electrical stimulus to evoke action potentials in the mechanoreceptive afferent. This study used mechanical stimuli which are more natural. Experimental results in my thesis can be related to the population response model of rapidly adapting fibers[3]. This is a probabilistic model where various types of stimulus parameters can be entered. In the model predictions, the number of active rapidly-adapting fibers was found to be important for intensity coding. The goal of this study is to make a comparison between psychophysical response and the somatosensory brain potentials evoked by the tactile stimuli. The working hypothesis is that certain stimulus parameter can be decoded from evoked potential data. This study can also provide more insight to studies about neuropathies and psychiatric conditions like autism which alters sensory perception. Since autism is classified as a pervasive developmental disorder that shows itself in abnormal social interaction, communication ability, patterns of interests, and patterns of behavior, the significance of such studies would be to find more about the neuropathology of autism regarding brain regions with sensory input and for basic processing of tactile information [4]. Additionally, this study can be of use in robotics for imitating the human tactile system.

2. BACKGROUND

2.1 Definition of the Psychophysics and Related Theory of Touch

The relation between stimulus and perception is examined with the scientific study called psychophysics, and therefore the problems of psychophysics are some of the most fundamental problems of neuroscience. Experimental stimuli that can be objectively measured, are employed and all the senses have been studied so far: e.g. vision, hearing, touch, taste, smell, and the sense of time. The three main topics in the realm of psychophysics regardless of the sensory domain, are listed as absolute thresholds, discrimination thresholds, and scaling[5].

A threshold, is the point of intensity at which the participant can just detect the presence of, or difference in, a stimulus. Stimuli with intensities below the threshold are usually considered not detectable, however stimuli at values close to threshold will often be detectable some proportion of the time [5]. Due to this, a threshold is considered to be the point at which a stimulus, or change in a stimulus, is detected some proportion p (75% in our experiments) of the trials.

The concept of an information-processing channel is fundamental to understand the properties of a sensory systems. A channel includes all the neural elements that are tuned to specific characteristics of the stimuli the system responds. Four information-processing channels (corresponding to four physiological receptors of tactile sensation) are thought to mediate the sense of touch. Their threshold curves are shown in Figure 1[6, 7, 8].

Each channel represents a certain receptor system. These receptor systems are named as NP I channel (Meissner receptors), P channel (Pacini corpuscles), NP II channel (Ruffini endings) and NP III channel (Merkel cells). Figure 1 the sensitivity thresholds of the four channels. By threshold, the amplitude of a vibratory stimulus

needed to induce sensation in a given amplitude at a certain frequency is implied. Therefore, according to Figure 1, at around 250 Hz the most sensitive channel is the P channel. To induce sensation in other channels, at the same frequency, the displacement must be increased. Similarly, at around 40 Hz the most sensitive channel is the NP I channel.

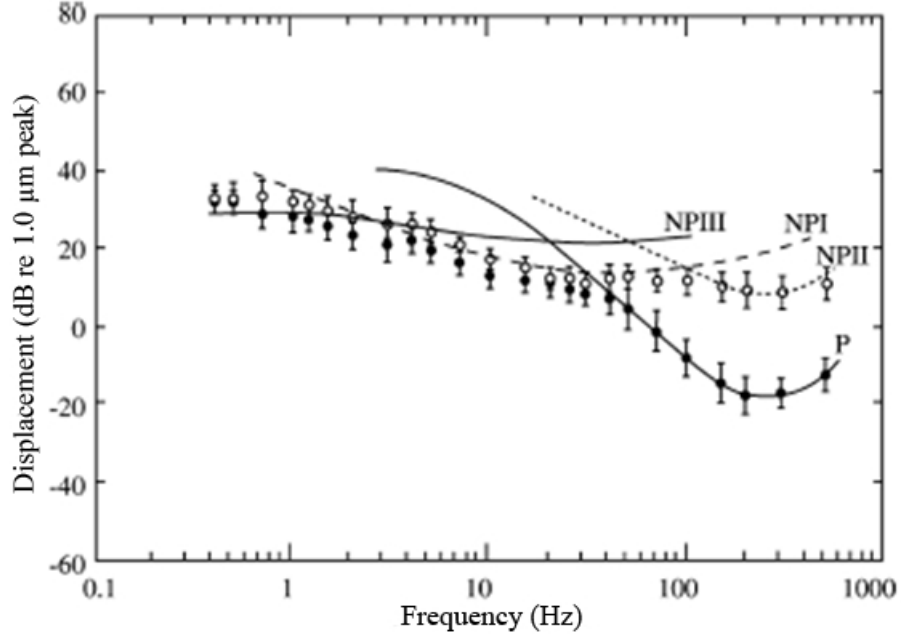


Figure 2.1 Four channel model of mechanoreception with extended frequency ranges of the tuning curves [8].

2.2 Somatosensory Evoked Potentials (SEPs)

Time-locked responses of the nervous system to external stimuli are evoked potentials (EPs). Somatosensory evoked potentials (SEPs) are one type of EP, which are generated by stimulation of afferent peripheral nerve fibers by electrical stimuli. By stimulating the skin at various dermatomal areas, SEPs can be recorded at various levels of the natural axis [9].

Clinical usage of the SEPs can be listed as Arm SEP, Leg SEP, SNAP, Trigeminal SEP, pudendal and bladder SEP, steady-state SEP to repetitive stimuli and finally Somatomotor SEP. Arm and leg SEPs are by far the most used of these. However,

mechanical stimuli such as vibrotactile stimuli can also be used to generate evoked potentials [10]. These are of course more natural stimuli, but their amplitudes have much lower amplitudes.

A normal response is shown in Figure-2. The waves identified in median nerve SEP's are EP, N13, N14, N18 and N20 which are also demonstrated in Figure 2. These waves are only obtained with electrical stimulus pulses.

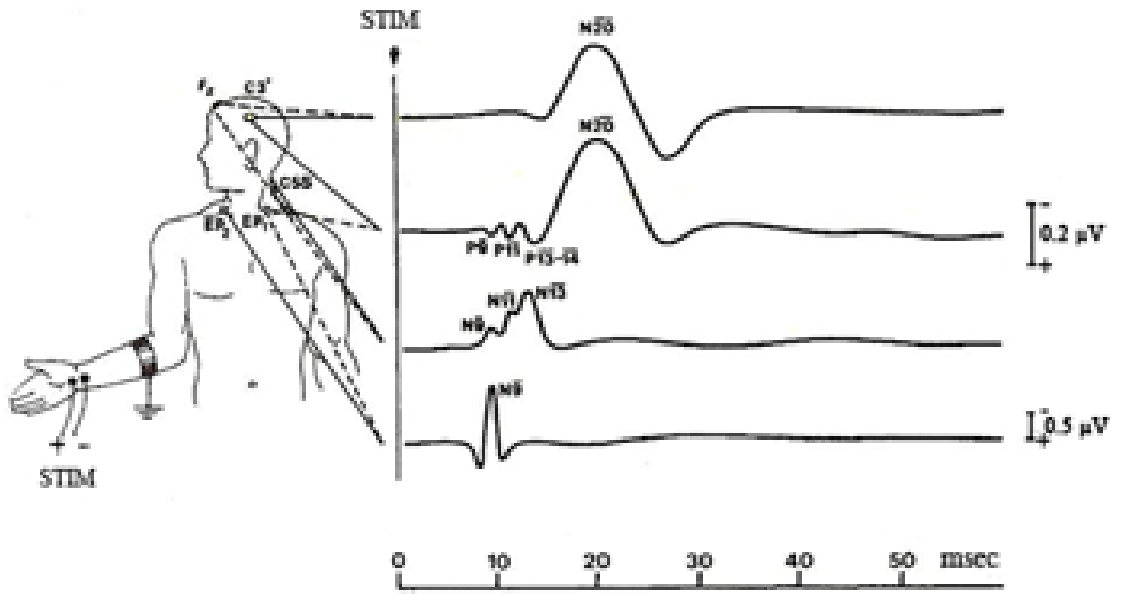


Figure 2.2 Somatosensory evoked potentials to arm stimulation [9]

SEPs are useful in studying disorders of the brain and brainstem, spinal cord, dorsal roots, and peripheral nerves. They are especially important to localize the anatomic site of somatosensory pathway lesions. SEPs may also be used to identify impaired conduction caused by axonal loss that are not disease specific. In addition, SEPs are useful in identifying clinically inapparent abnormalities and lesions causing only vague or equivocal signs or symptoms, and offer a noninvasive, often quantifiable method of assessing known lesions. SEPs may also be useful in certain conditions in which the diagnosis is uncertain, by indicating involvement of central somatosensory pathways, as well as suggesting the type of involvement (e.g., demyelination)[11].

2.3 Anatomy of Skin and Mechanoreceptors

Skin is the largest organ of the human body. The sensory receptors are responsible for tactile sensation are located in this multilayered organ. It is highly complex that it incorporates not only epithelial cells, the mechanoreceptors and nerve fibers, but also blood vessels, sweat glands and other specialized structures.

Skin is classified into two major types, which have its own complement of receptors specialized to mechanical stimulus and internal structure. These are called glabrous skin or hairless skin that covers the surface of our palm and the soles of the feet and hairy skin that is the source of our body hair. There is also a transition skin type called the mucocutaneous skin which lines the entrance to the inside of the body[12].

The electrophysiological experiments show that there are four types of tactile afferent fibers innervating the glabrous skin [2]. These are fastly adapting Type I fibers (FA I or RA), Pacinian fibers (PC or FA II), slowly adapting Type I (SA I) and slowly adapting Type II (SA II) fiber.

There are two principle properties help to classify that these four types of mechanoreceptive fibers. : adaptational properties and receptive field size. SAI and SAII are slowly adapting whereas the other two are FAI (or RA) and FAII (or PC) are fast adapting [2, 12, 13, 14]. The adaptation here refers to how these afferent fibers respond to a sustained skin indentation. Figure 3 shows that mechanoreceptors in glabrous skin vary in the size and structure of their receptive fields[15].

Meisner's and Pacinian corpuscles are FA or fastly adapting, they tend to respond quickly at first but then stop firing action potentials, even though the stimulus continues. Merkel's disks and Ruffini's endings are SA or slowly adapting, they generate acontinuous train of action potentials with long duration stimulus (Figure 4) [13].

Variations among somatic sensory receptors of the skin in receptive field size

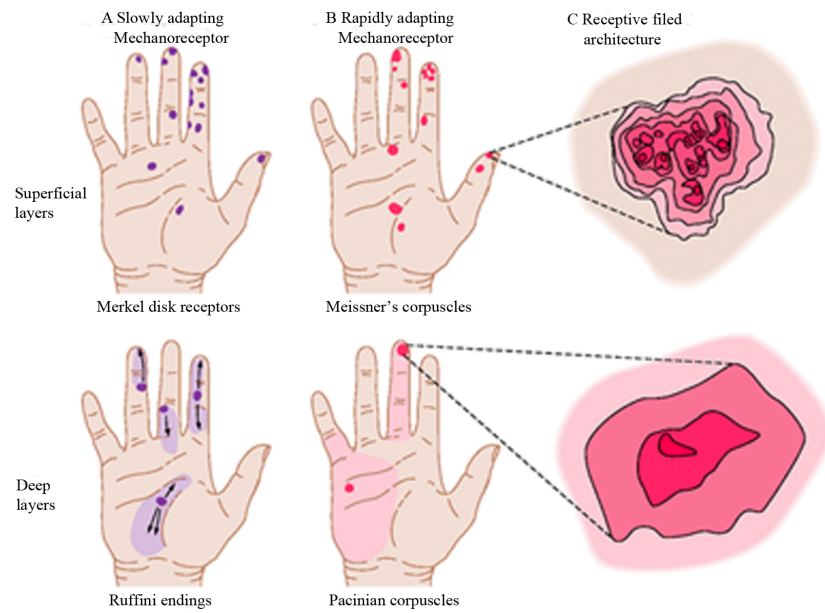


Figure 2.3 Mechanoreceptors in the glabrous skin and the structure of their receptive field.[15]

and adaptation rate [1]. It is very important that the previous studies especially about rapidly adapting fibers of cats and Meissner Corpuscles, there observed a reliable mathematical connection between physiology and psychophysics [14, 16, 17]. Therefore, it is possible to examine that total neuron activity and psychophysical behaviour [15, 18, 19] Figure 4 below summarize the receptive field size and the adaptation property for four mechanoreceptors of the skin.

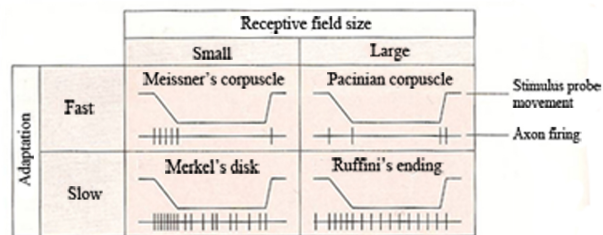


Figure 2.4 Variation among somatic sensory receptors of the skin in receptive field size and adaptation rate.[1]

2.3.1 Vibration Sense and Mechanoreceptors

Vibration is the sensation produced by oscillations of objects positioned close of the skin. The hum of an electric motor, the strings of a musical instrument or tuning fork used in the neurological examination are examples of the vibration sources. Mechanoreceptors in the skin react to oscillations by a pulse code and the sensory nerves fire an action potential per each cycle of the oscillation if its amplitude is high. In Figure 5 this pulse code relation is demonstrated.

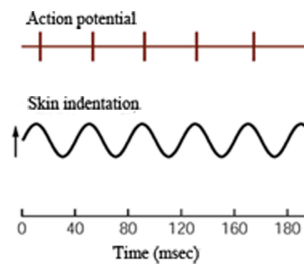


Figure 2.5 A rapidly adapting mechanoreceptor responds to sinusoidal mechanical stimuli with a single action potential for each cycle [15].

Each mechanoreceptor has different threshold sensitivity to vibration. Merkel disk receptors are most responsive to low frequencies (5-15Hz) whereas Meissner's corpuscles are most susceptible to midrange stimuli (25-50Hz) and the Pacinian corpuscles have the lowest thresholds for high frequencies (60-400Hz). The Pacinian corpuscles can detect vibrations smaller than $1\mu\text{m}$ at 250 Hz; however, they require stimuli with much larger amplitudes at 30 Hz [15-19]. Figure 6 presents the frequency sensitivity of two fastly adapting tactile fibers of the skin.



Figure 2.6 Frequency sensitivity of two fastly adapting tactile receptors of the skin [15].

2.3.2 Mechano-electric transduction

Mechanical energy applied to the skin are converted by the various tactile mechanoreceptors into electrochemical energy used by the nervous system [12]. This

mechanism was studied by performing experiments on Pacinian corpuscles isolated from the mesentery of the cat, which are anatomically and physiologically similar to those located within human skin. It is commonly accepted that the mechanisms of transduction found for the Pacinian corpuscles are common to the other tactile receptors. Figure 7 depicts the schematic diagram defining the various components forming the Pacinian corpuscle.

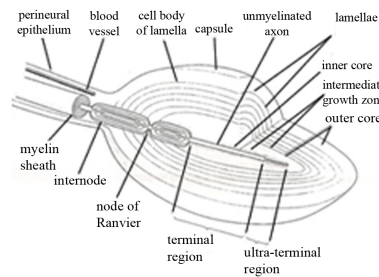


Figure 2.7 Pacinian Corpuscle schematic diagram illustrated with its components [12]

Mechanotransduction typically works in the following way. When a mechanical stimulus is applied to the receptor, either via the skin directly, the accessory structure acts as a mechanical filter, transmitting the applied strain to the unmyelinated transductive membrane. The strain at the level of the mechanosensitive membrane induces hypothesized strain (stretch) sensitive channels to respond by increasing their conductance to certain ions, Na^+ ions in particular, although a contribution from K^+ ions may also occur. The electrochemical forces on ions are such that sodium ion channels increase their conductance then Na^+ will rush into the neuron, causing depolarization. The increase in conductance as a result of activating strain-sensitive channels is evidenced by the transmembrane electrical event known as receptor potential. If the receptor potential is sufficient in amplitude, an action potential will be generated and propagated along the peripheral nerve to locations within the central nervous system.

2.4 Primary Afferent Axons

The skin is richly innervated by axons that course within the vast network of peripheral nerves on their way to the CNS. Axons bringing information from the

somatic sensory receptors to the spinal cord or brain stem are the primary afferent axons of the somatic sensory system. The primary afferent axons enter the spinal cord through the dorsal roots; their cell bodies lie in the dorsal root ganglia as depicted in Figure 8 [15].

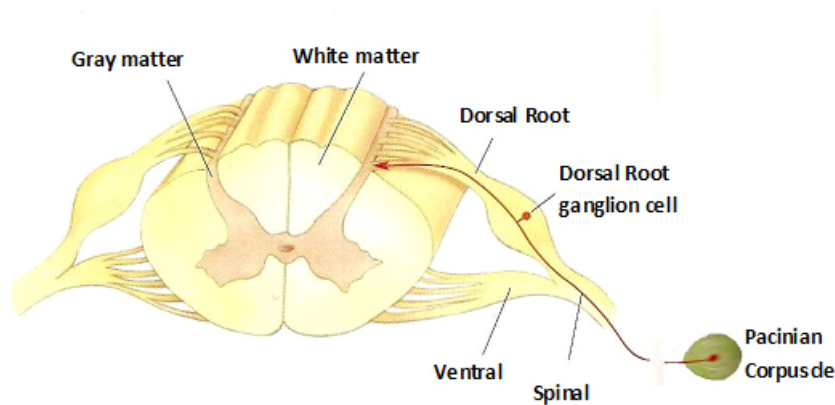


Figure 2.8 Structure of a segment of the spinal cord and its root. [1]

2.5 Dorsal Column-Medial Lemniscal Pathway

The dorsal column medial lemniscal system is the principal pathway for perception of touch and proprioception. The organization of this pathway is summarized in Figure 9. The ascending branch of the large sensory axons enters the ipsilateral dorsal column of the spinal cord, the white matter tract medial to the dorsal horn. The dorsal columns carry information about tactile sensation and limb position toward the brain. They are composed of primary sensory axons and second order axons from neurons in the spinal gray matter. The axons of the dorsal column nuclei ascend within a conspicuous white matter tract called medial lemniscus. It rises through the medulla, pons, and midbrain, and its axons synapse upon neurons of the ventral posterior (VP) nucleus of the thalamus. No sensory information goes directly into the neocortex without first synapsing in the thalamus. Thalamic neurons of the VP nucleus then project to specific regions of primary somatosensory cortex or S1 [1]. The functional and anatomical organization of sensory processing networks is hierarchical.

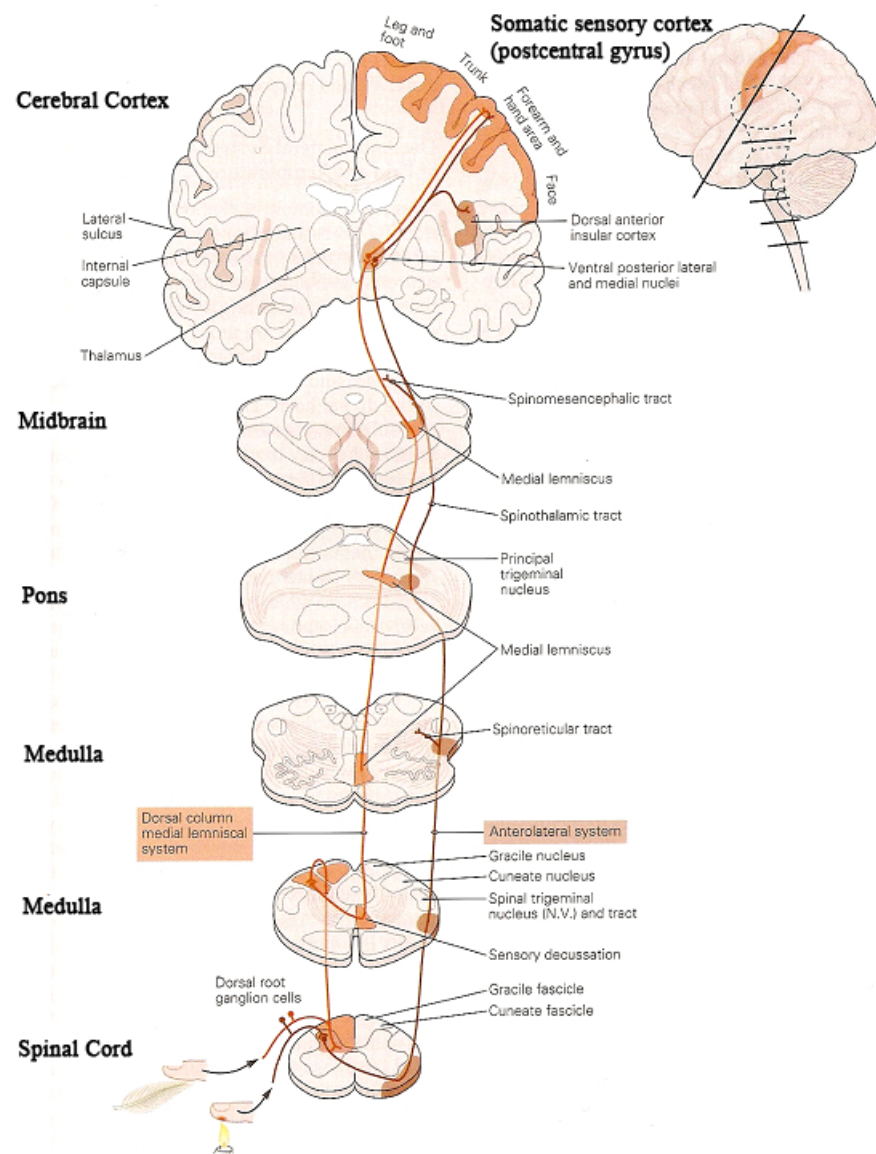


Figure 2.9 Sensory information from limbs and trunk [15]

Stimulation of a population of receptors initiates signals that are transmitted through a series of relay nuclei to higher centers in the brain (only one relay is shown in following Figure 10). At each processing stage the signals are integrated into more complex sensory information[15].

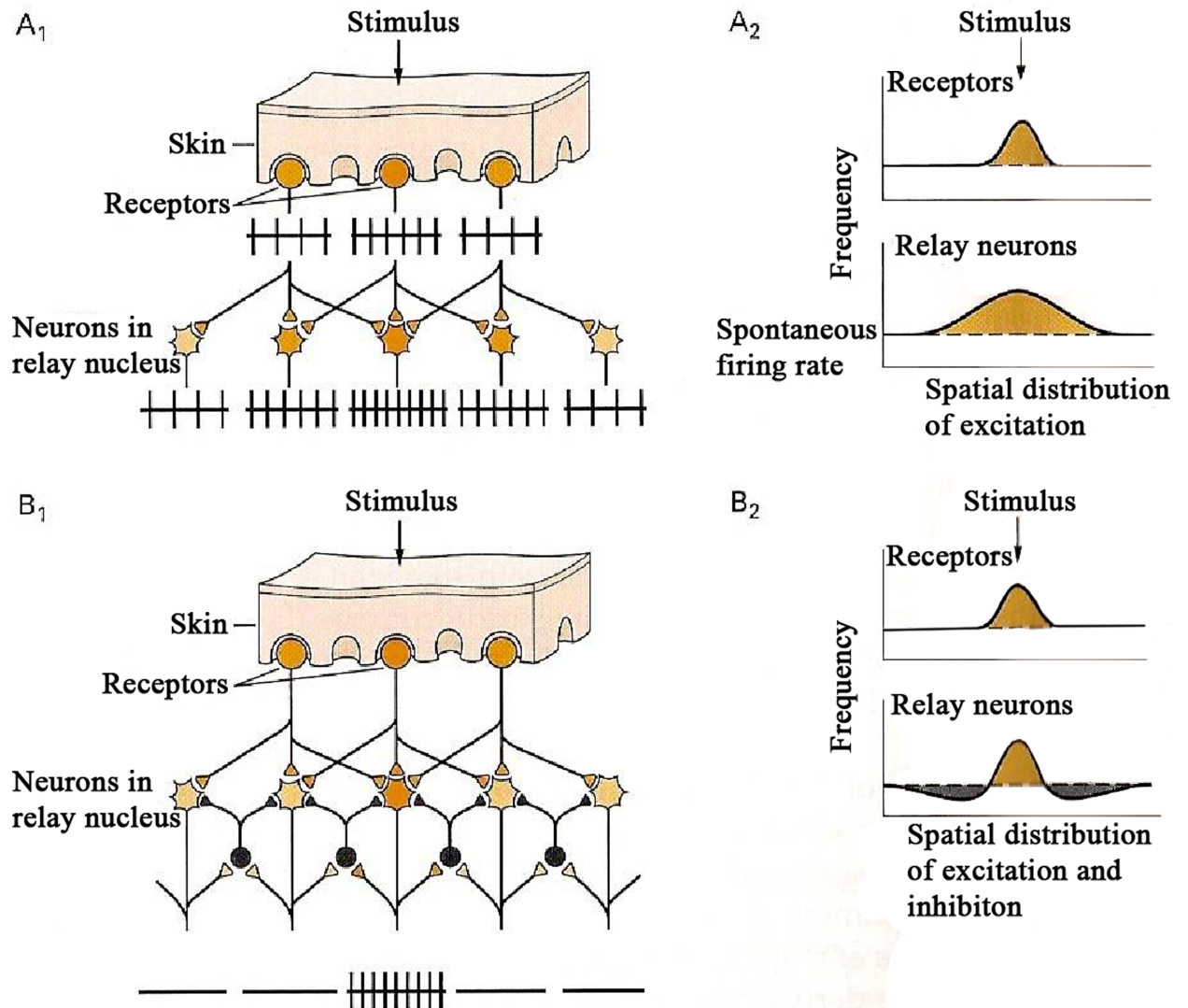


Figure 2.10 The functional and anatomical organization of sensory processing networks .[15]

A. In the somatosensory system excitatory synaptic connections from each receptor in the skin are widely distributed to a large group of postsynaptic neurons at

each relay nucleus. 1- Each relay neuron receives sensory input from a large group of receptors and therefore has a bigger receptive field than any of the input neurons. 2- Receptors closest to the stimulus respond more vigorously than distant receptors. B. 1. The addition of inhibitory interneurons (gray) narrows the discharge zone. 2- On the either side of the excitatory region the discharge rate is driven to the resting level by feedback inhibition[15].

2.6 Somatosensory Cortex

The primary somatic sensory cortex integrates information about touch. In series of relay regions within the brain, the sensory organization processed. Mechanoreceptors in the skin send their axon to the caudal medulla, where they terminate in the gracile or cuneate nuclei. Through the dorsal column-medial lemniscal pathway the sensory information reaches finally to the somatosensory cortex. The somatic sensory cortex has three major divisions: the primary and secondary somatic cortices and the posterior parietal cortex. Figure 11 is the illustration of the somatic sensory areas of the cortex.

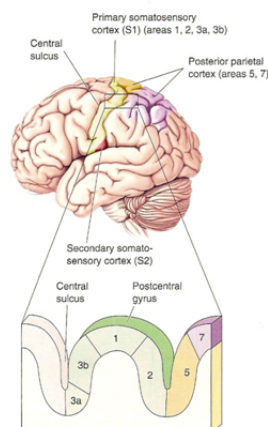


Figure 2.11 Somatic sensory areas of the cortex. [1]

Each region of the somatic sensory cortex receives inputs from primarily one type of receptor as it can be seen from the Figure 12. From the Figure 12, part A, the four regions of the somatic sensory cortex-Broadmann's areas 3a, 3b, 1, and 2 inputs

from one type of receptor from specific parts of the body are organized in columns of neurons that run from the surface to the white matter. B represents the detail columnar organization of inputs from digits 2,3,4 and 5 in a portion of Brodmann's area 3b. Alternating columns of neurons receive inputs from rapidly adapting RA and slowly adapting SA receptors in the superficial layers of skin. Figure C shows the overlapping receptive fields from RA and SA fibers which project to distinct columns of neurons in area 3b.

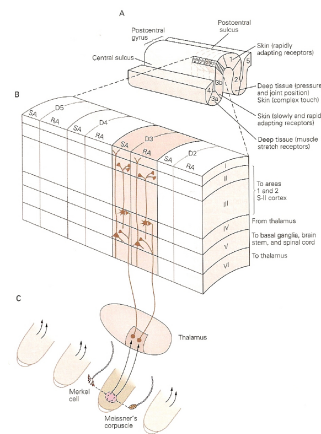


Figure 2.12 Input pathway of sensory cortex from primarily one type of receptor. [15]

2.6.1 Primary Somatosensory Cortex

Primary somatic cortex S-I contains four cytoarchitectural areas: Brodmann's areas 3a, 3b, 1, and 2. Most thalamic fibers terminate in areas 3a and 3b, and the cells in areas 3a and 3b project their axons to areas 1 and 2. Thalamic neurons also end in small projection directly to Brodmann's areas 1 and 2. Functionally, these four areas vary [19]. Areas 3b and 1 receive information from receptors in the skin, whereas areas 3a and 2 receive proprioceptive information from receptors in muscles and joints. However, the four areas of the cortex are widely interconnected, so that both serial and parallel processing are involved in higher-order elaboration of sensory information. [1] Principly, projections from the SI are required to function of area secondary somatosensory cortex-SII. In contrast, removal of SII has no effect on the response of neurons in SI. SII cortex projects to the insular cortex, which in turn

innervates regions of the temporal lobe believed to be significant for tactile memory [19].

2.7 Frequency Following Responses

Dependency of the evoked response to vibrotactile stimuli, the frequency following response (FFR), is a predictable phenomenon in which the human brain has a tendency to change its dominant EEG frequency towards the frequency of the external stimulus. This may arise from the synchronous firing of many cortical neurons. Neural responses to vibrotactile stimuli are specifically expressed in the form of FFR, clearly entrainment of discharge activity at the driving frequency and also its low harmonics[20, 21]

3. METHOD

3.1 Subjects

Five female and five male subjects who had no physiological or psychological disorders were recruited. These subjects came from a young age group ages of 22-30, since vibrotactile sensitivity decreases with age [3]. The experiments adhered to NIH ethical guidelines for testing human participants and were approved by the Ethics Committee for Human Subjects of Boğaziçi University.

3.2 Experimental Setup

3.2.1 Apparatus

Stimuli were generated by a computer and amplified. The amplified stimuli were applied to the left middle fingertip by a V203 electro-dynamic shaker driving a contactor probe with 2mm radius and no contactor surround (Ling Dynamic Systems Ltd., Royston, Herts, UK). The shaker was mounted on a horizontal metal rail and will be vertically lowered to the fingertip. The vibrations generated by the shaker were measured by LVDT (Lucas Control Systems, Pennsauken, NJ) and monitored with an oscilloscope. In order to prevent the movement of the fingertip, the finger was immobilized in modeling clay. The fingertip was also monitored by a CCD camera. The sound of the shaker was masked by continuous auditory noise applied with headphones. The response of the subject was obtained by a custom-made response box connected to the computer. EPs were recorded by a portable evoked-potential amplifier (Micromed System Plus).

3.2.2 Stimuli

The stimuli were mechanical vibrations which started and ended as cosine-squared ramps of 50ms rise/fall times. The duration of the test stimuli was 0.5s. The stimuli were burst of sine waves in envelopes of different amplitudes as shown in Figures 13. The interval between two stimuli was 2 seconds.

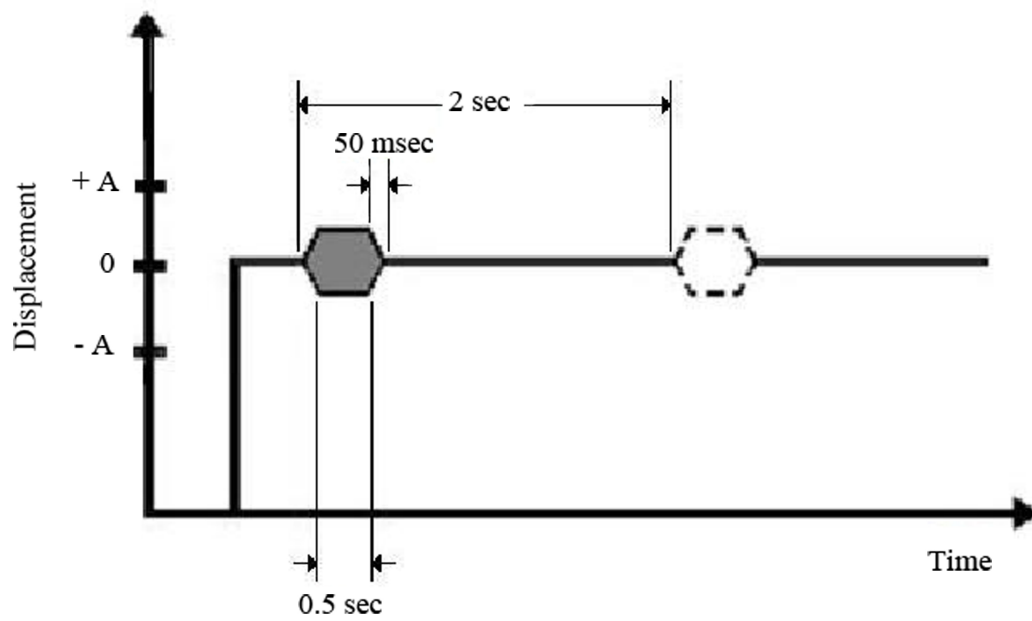


Figure 3.1 Stimulus timing diagram for the two-interval forced-choice task

3.3 Experimental Protocol

The experiment was composed of two parts. In the first part, psychophysical thresholds (unmasked) of each subject was determined at six frequencies (2, 10, 40, 100, 250 Hz & 500 Hz). In the second part, SEPs were recorded at various stimulus intensities related to the P channel frequencies were 230Hz and 40Hz.

3.3.1 Part I

In all the psychophysical threshold experiments, the two-interval forced-choice task was used to obtain results independent of the subject's criterion. The stimulus levels were changed by an up-down rule [3] which had the level of stimulus increased by one step (1 dB) for each incorrect answer; and decreased one step (1 dB) for three correct answers which were not necessarily consecutive. The threshold experiment was stopped automatically when the subject's responses varied within ± 1 dB range for the last 20 trials. The stimulus level at the end of this procedure was recorded as the threshold. The time intervals of the two-interval forced-choice task were presented to the subject by red and green lights on the response box. At the end of each trial, a yellow light on the box signaled that a response was expected from the subject. In this part of the experiment, the subject's task was to decide whether the stimulus occurred in the first or the second interval. The stimuli consisted of bursts of sine waves with a static indentation of 0.5mm [20;21]. The static indentation is important since thresholds may be affected by it [3]. After a contact with the skin was achieved, the static indentation was adjusted by a micrometer. Each threshold measurement session for a given frequency was repeated four times (Figure 13).

3.3.2 Part II

Part II consisted of evoked-potential recordings. In this part, first a test recording was done to check the subject if he or she had a problem in the path of median nerve with traditional electrical stimuli applied on the wrist. The electrode positions were CPi(+) and CPc(-). A major peak N20 was generated by thalamocortical radiations or the cerebral cortex [10]. Contact impedances of the electrodes were below 5k Ω . Mechanical stimuli which were identical to those used in Part I applied while recording evoked potentials. For each tested frequency (40 Hz and 230 Hz), three recordings were obtained at each stimulus amplitude. Frequency Following Responses were recorded from the area SI on the scalp when mechanical vibrations were applied to third digit at left hand. Positive electrode (+) of amplifier were connected to point CPc and negative

electrode of amplifier were connected to the point CPi. Potentials were averaged at 500 times. Resulted time series were filtered between 10-160 Hz and 60-1000 Hz fourth degree Butterworth band-pass filter for 40 Hz and 230 Hz stimulus respectively.

3.4 Analysis

For the first part, each measurement on every subject was repeated four times. The averages of the four measurements were calculated for further analysis. T-tests was applied to the raw data to test the statistical differences between subjects' responses. For the second part, EPs recordings were filtered and averaged to reduce the noise. Grand averaged and averaged responses were analyzed with Wavelet Transform in MATLAB software. Some data were not included the average due to obtaining artifacts. (artifact : $V > 1\mu V$)

3.5 Wavelet Transform

Thanks to the wide variety of signals and problems encountered in medicine and biology, the spectrum of applications of the wavelet transform (WT) is tremendously outsized. Wavelet transform used in the analysis of the more traditional physiological signals (e.g: the electrocardiogram or briefly ECG) and its range is extended to the very recent imaging modalities (e.g: positron emission tomography (PET), magnetic resonance imaging (MRI)) [22]. Continuous wavelet transform (CWT), with the ability to preserve phase information, is usually adopted for harmonic analysis [23].

The Fourier transform can be utilized to quantify oscillation amplitude across the entire frequency spectrum. Yet, the Fourier transform holds no temporal information. To preserve some temporal information, the Fourier transform can be applied to the consecutive EEG segments labeled by a windowing function ('short-term Fourier transform' or 'windowed Fourier transform'). Similar to Heisenberg's uncertainty prin-

ciple, the width of the windowing function describes together the temporal and the frequency resolution of this method. Since The windowed Fourier transform uses a fixed and arbitrarily defined window width, the resulting resolution has a fixed time-frequency pattern. In case of defining a narrow window, temporal resolution will be high (i.e., it will be promising to resolve the occurrence of timely closer two events) whereas the frequency resolution will be low (i.e., it will not be possible to determine the occurrence of two events that are closer in frequency). On the opposite, when defining a large window, the frequency resolution of the transform will be high, but at the cost of a low temporal resolution[24]. However, in wavelet analysis there is no a fixed window width and have high resolution in time and frequency that can be attained (Figure 14). Specifically $\sigma_t \sigma_\omega$ must be greater than or equal to $\frac{1}{4\pi}$. If it is verified in the time domain and frequency domain and integrating their squared modulus leads to $\sigma_t = 1/\sqrt{2}$ and $\sigma_f = \sqrt{2}/4\pi$ [25].

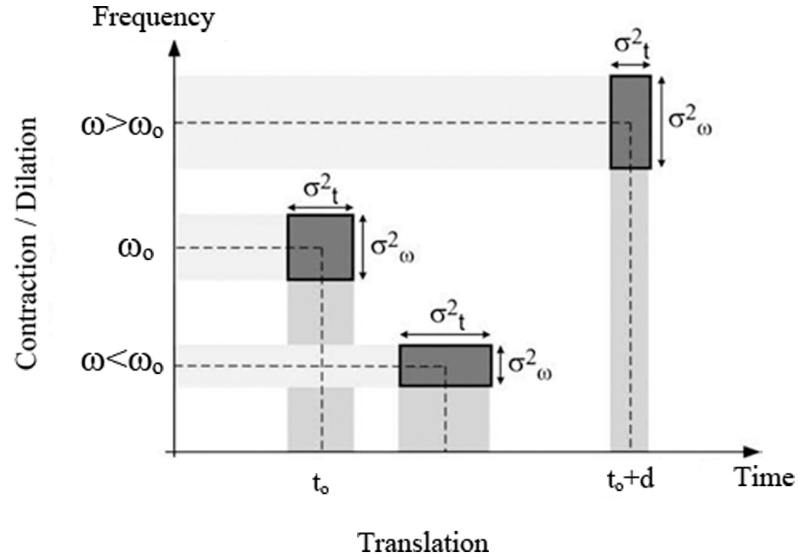


Figure 3.2 Heisenberg Boxes; Time-frequency diagram of the wavelet transform. Representation of the window width which have simultaneous resolution in the time and frequency in wavelet transform [24].

Complex Morlet Wavelet has a feature that offers better results in the case of decomposing noisy signal envelopes [24]. Most commonly employed Complex wavelet is the Morelet wavelet, that is described as

$$\psi(t) = \sqrt[4]{\pi} (e^{i2\pi f_0 t} - e^{-\frac{(2\pi f_0)^2}{2}}) e^{-\frac{t^2}{2}} \quad (3.1)$$

where f_0 is the central frequency of the mother wavelet as it refers to the frequency location of the morelet wavelet. The second term in the brackets is recognized as the correction term. The term corrects the non-zero mean of the complex sinusoid of the primary term. In practice, it turns into a negligible term for the values of the $f_0 \gg 0$ and can be disregarded if the Morelet wavelet can be written in simpler form as [25] :

$$\psi(t) = \frac{1}{\pi^{1/4}} e^{i2\pi f_0 t} e^{-\frac{t^2}{2}} \quad (3.2)$$

Fourier transform of the Morelet wavelet is given by

$$\hat{\psi}(t) = \pi^{1/4} \sqrt{2} e^{\frac{1}{2}(2\pi f - 2\pi f_0)^2} \quad (3.3)$$

To construct the dilated and translated Morelet wavelet t is replaced with $(t-b)/a$. Its form then

$$\psi\left(\frac{t-a}{b}\right) = \frac{1}{\pi^{1/4}} e^{i2\pi f_0 \left(\frac{t-a}{b}\right)} e^{-\frac{\left(\frac{t-a}{b}\right)^2}{2}} \quad (3.4)$$

4. RESULTS

4.1 Psychophysical Thresholds

Absolute thresholds of 10 subjects were measured for 6 different test frequencies from the middle phalanx were obtained. Figure 15 shows results that are averaged across the subjects. The results found in this were mostly similar to the values found by Bolanowski et al 1988.

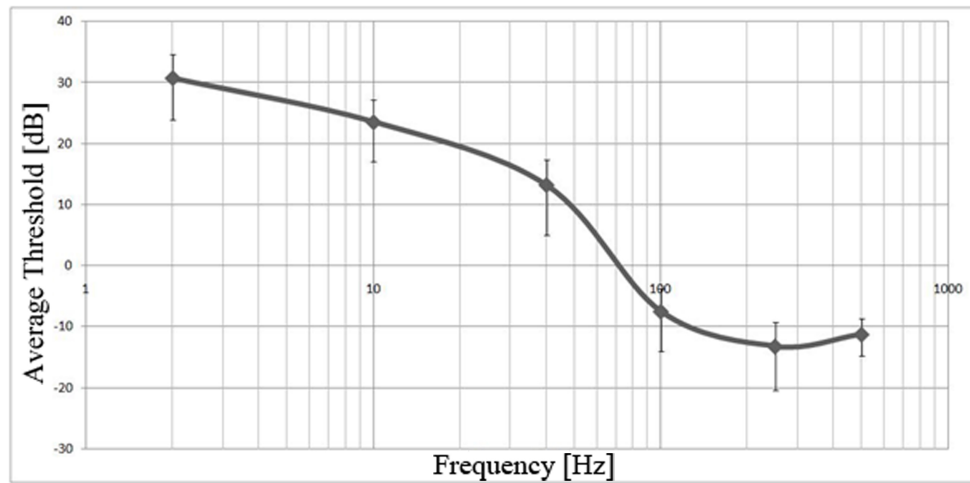


Figure 4.1 Psychophysical thresholds.

4.2 Somatosensory Evoked Potentials

In this part subject's SEPs were tested to confirm there were no physiological problems. This was performed by electrical stimulation of the median nerve. Figure 16 shows that there is negativity before 20 msec. which can be defined as the negative peak N(20) reported in the literature. All individuals were found to be healthy in this respect. (For all subjects recordings see Appendix B).

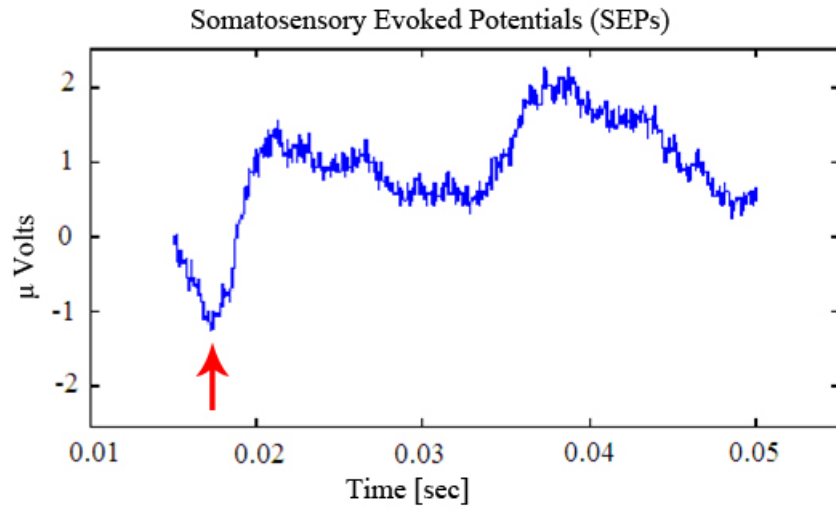


Figure 4.2 Somatosensory Evoked Potentials recorded from 1 subject.

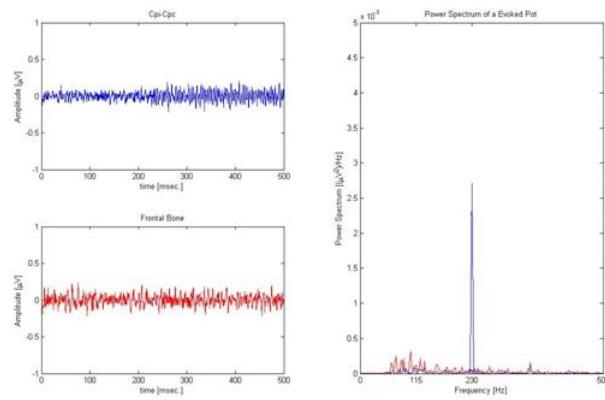


Figure 4.3 Psychophysical thresholds.

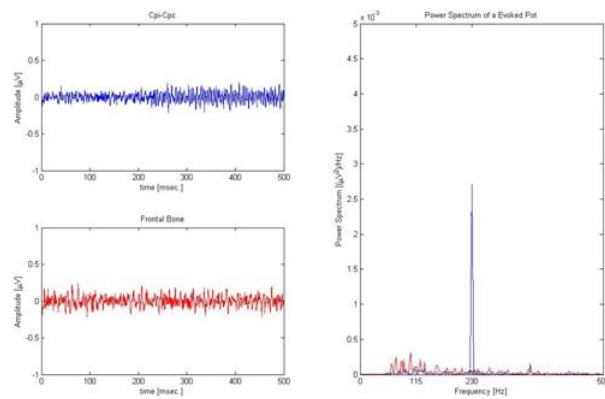


Figure 4.4 Psychophysical thresholds.

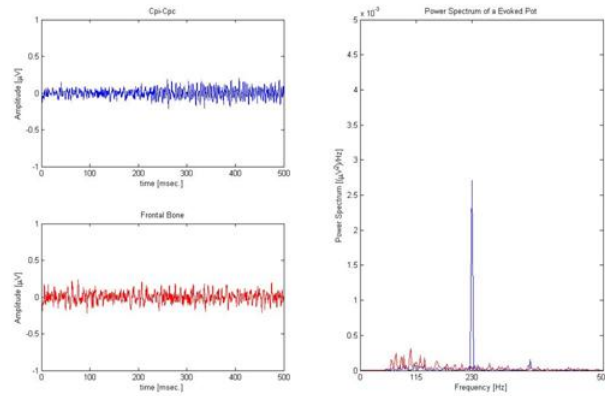


Figure 4.5 Frequency following response recorded from SI of one subject evoked by mechanical vibrations at 40 Hz frequency and (A) 10 dB SL (B) 20 dB SL (C) 30 dB SL amplitude.

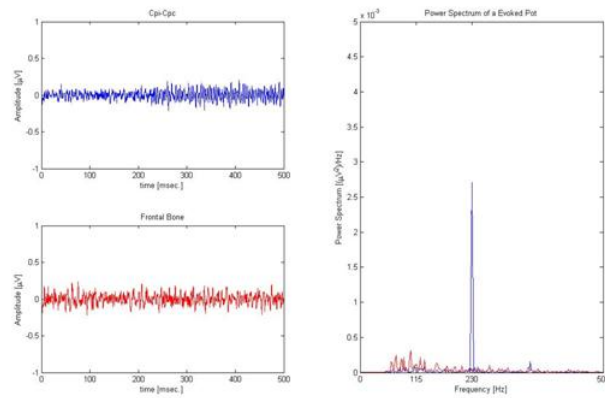


Figure 4.6 Psychophysical thresholds.

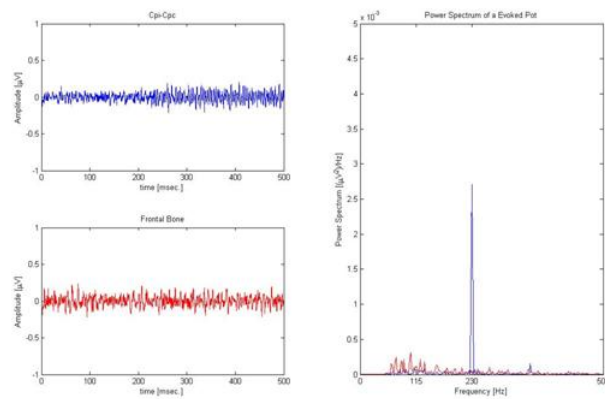


Figure 4.7 Psychophysical thresholds.

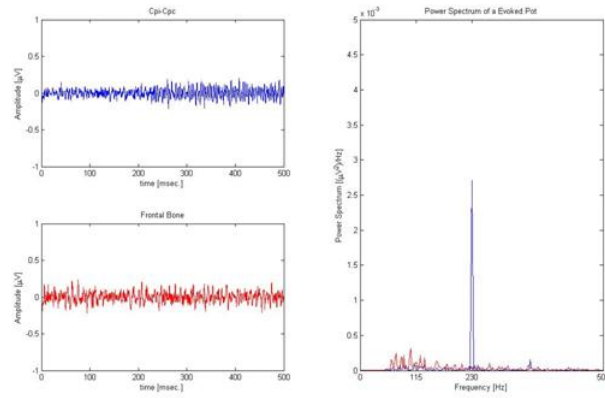


Figure 4.8 Frequency following response recorded from SI of one subject evoked by mechanical vibrations at 230 Hz frequency and (A) 10 dB SL (B) 20 dB SL (C) 30 dB SL amplitude

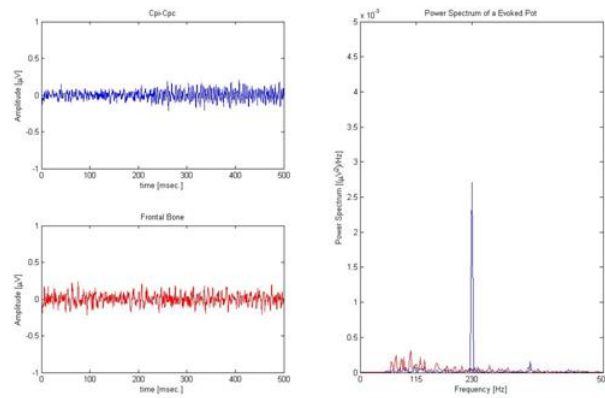


Figure 4.9 Psychophysical thresholds.

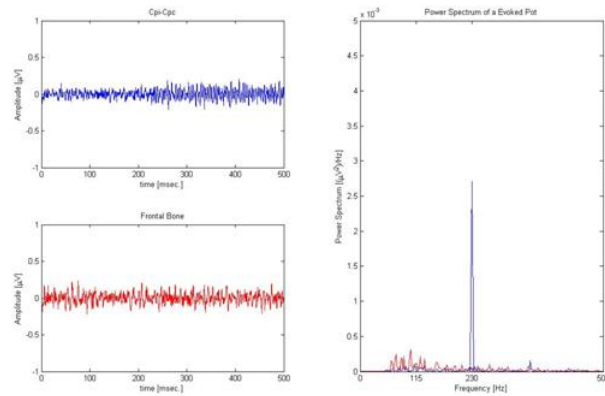


Figure 4.10 Psychophysical thresholds.

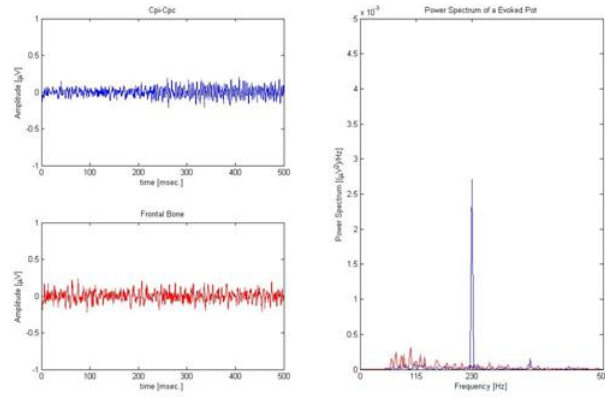


Figure 4.11 19 Frequency following response recorded from SI of one subject evoked by mechanical vibrations at 40 Hz frequency and (A) 10 dB SL (B) 20 dB SL (C) 30 dB SL amplitude. (A) averaged for 8 subjects, (B) averages for 6 subjects and (C) averages for 5 subjects.

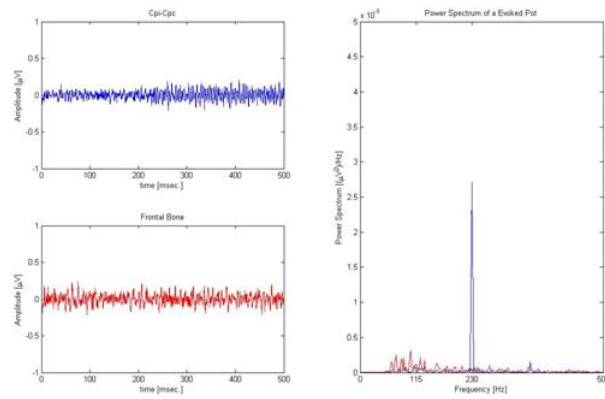


Figure 4.12 Psychophysical thresholds.

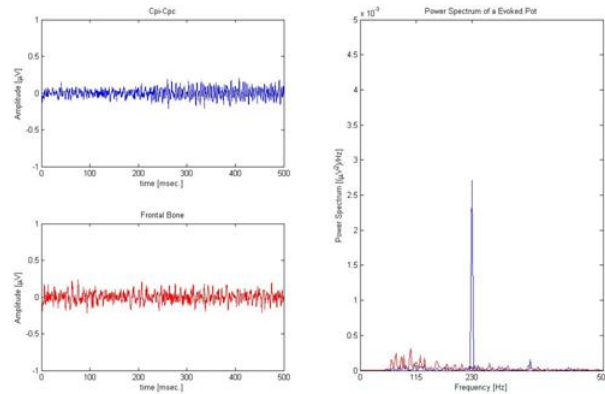


Figure 4.13 Psychophysical thresholds.

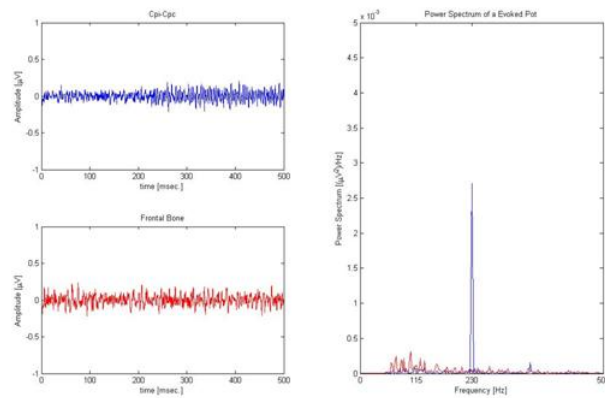


Figure 4.14 19 Frequency following response recorded from SI of one subject evoked by mechanical vibrations at 40 Hz frequency and (A) 10 dB SL (B) 20 dB SL (C) 30 dB SL amplitude. (A) averaged for 8 subjects, (B) averages for 6 subjects and (C) averages for 5 subjects.

5. DISCUSSION

In addition to frequency-following responses, low frequency (10-20 Hz) brain oscillations have been seen in the recordings. These oscillations are included in the alpha and beta EEG bands. However, when the mechanical stimuli were applied, the background activity decreased and during the first half of the stimulus significant activity re-occurred between 10-20 Hz. The 30 dB SL amplitude stimulus is a high amplitude for the peripheral afferent and almost all neurons' action potentials are frequency locked to this stimulus cycle [16]. My findings show that afferent synchronization occurred and subharmonic may occur because of imperfect synchronization[14, 16, 17].

Figure 20 includes evoked potentials' time-frequency graphics recorded from primary somatosensory cortex while mechanical stimulus at 230 Hz frequency was applied during 0.2-0.5 sec. These graphs can be discussed in the same manner with the previous plots. It was observed that, at this high frequency stimulation signal to noise ratio is less. In addition, when 30 dB SL amplitude stimuli was applied brain oscillations at the same frequency with stimuli were observed.

The following Figure 21-22 present the control recordings stimulus at 40 and 230 Hz. Another set of two electrodes were connected to the forehead as a second channel to test whether original recordings were mechanical or electrical artifacts.

As it can be seen from the Figure 20-21 prominent peaks are produced at the same frequency during 40 Hz and 230 Hz stimulus only by the SI. This demonstrates that there was no mechanical or electrical artifacts in my experimental setup. Paired t-test results showed that there was a significant increase in frequency locked responses, for both frequencies when the stimulus intensity increased [16].

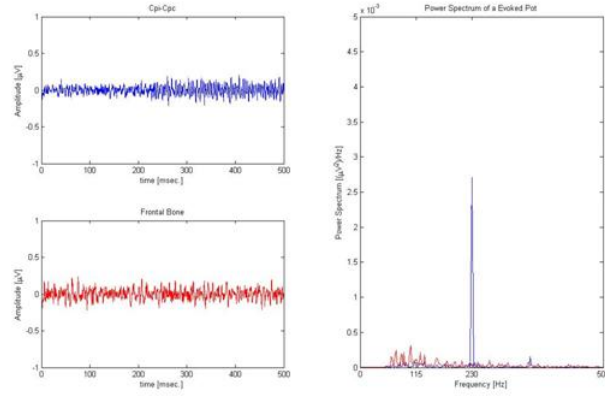


Figure 5.1 Control recordings for the 40 Hz evoked potentials. Left column: evoked potentials raw data, right column: power spectrum density. Red and blue lines represents control channel and CPi-CPc respectively.

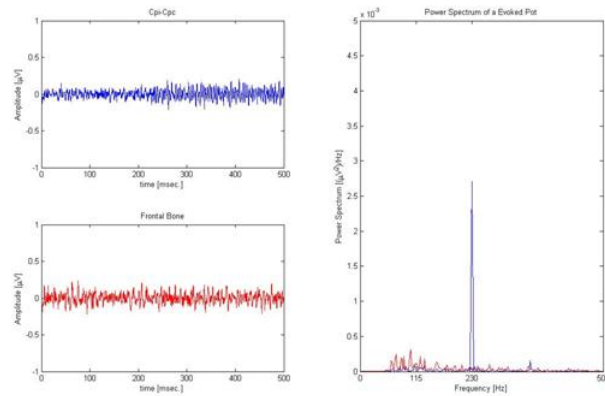


Figure 5.2 Control recordings for the 230 Hz evoked potentials. Left column: evoked potentials raw data, right column: power spectrum density while the stimulus were applying. Red and blue lines represents control channel and CPi-CPc respectively.

6. CONCLUSION

During 40 Hz stimuli, cortical potentials may occur once every cycle (40 Hz) or every other cycle (20 Hz) This fact was not previously shown. Cortical activity decreasing before the stimulus ends may be due to a central adaptation process. Increased concentration of activity observed at frequency space due to an increase in the stimulus amplitude is supported by the findings in the literature.

During 230 Hz at the 30 dB SL intensity, I observed that brain oscillations have the identical frequency as the peripheral stimulus in the same subject. This finding suggests almost complete frequency locking for the P channel. It was also observed that for a 40 Hz stimulation stimuli with three different intensities clearly produced frequency locking. However, when all signals from different subjects were averaged, these conclusions became more blurry.

To sum up, Fourier transform and wavelet transform plots show that the background activity is suppressed and the frequency-following activity increases during the stimulus period increased as the mechanical stimulus intensity increases These results were statistically significant The origin of frequency-following responses may be explained based on single-unit recording.

7. Limitations of the Study

In this study, subjects were human, so non-invasive evoked potential recordings were used. The results were in less than 1 micro volt, therefore they were very hard to record. Noise was reduced by averaging and filtering. Increasing the sample size may reduce some of the variance in data.

Anatomical differences for locating SI may have affected the results. In some sessions movement artifacts were observed, this may be caused because of the lack of comfort of the subjects during records.

8. Future Work

In my study, frequency following responses were tested for 40 Hz mechanical stimulus which activates the Non-pacinian I or Pacinian channel and 230 Hz mechanical stimulus which activates the P channel. The results are important to construct computational models. For the further studies similar experiments can be performed with needle electrodes on animal's scalp or surface electrodes on exposed cortex. This would increase signal-to-noise ratio. Frequency-following responses may be important to understand psychophysical masking.

APPENDIX A. APPENDIX A

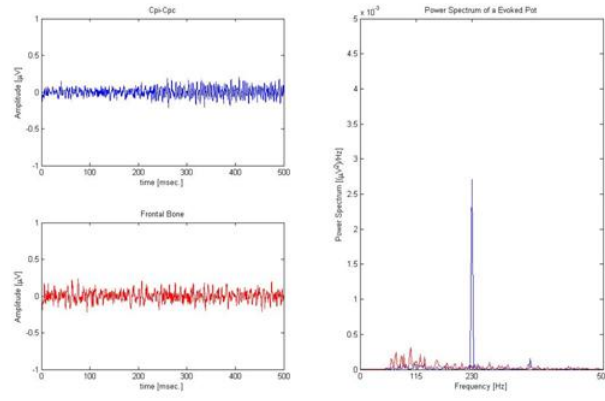


Figure A.1

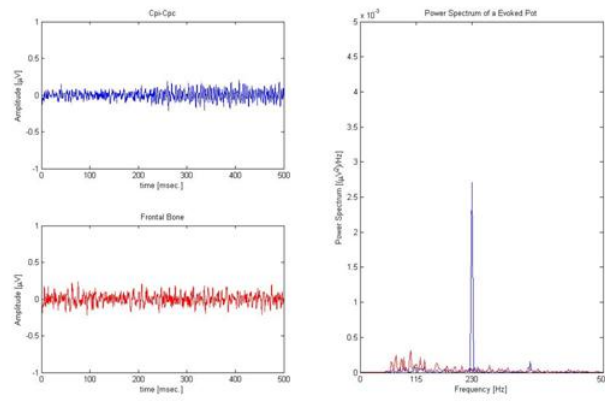


Figure A.2

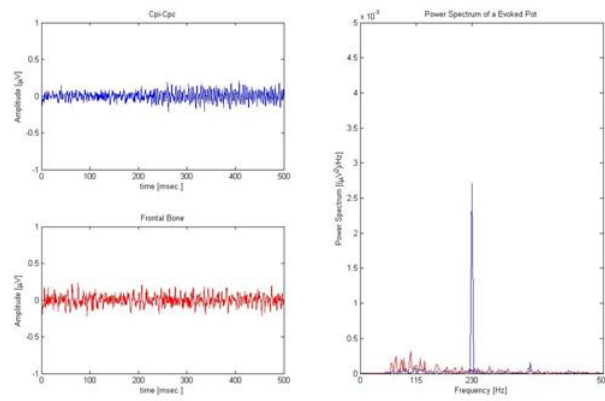


Figure A.3

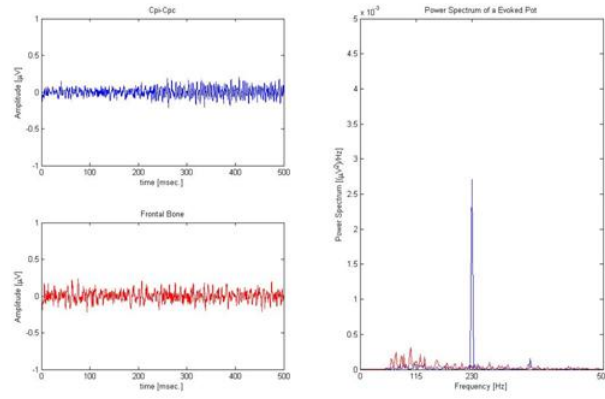


Figure A.4

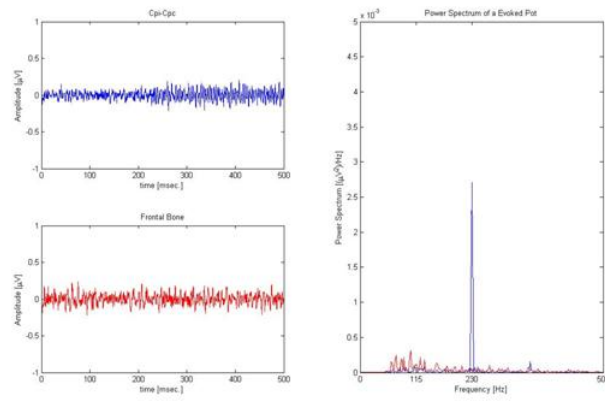


Figure A.5

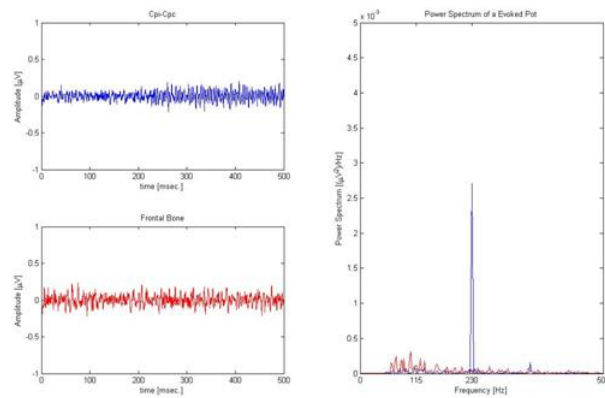


Figure A.6

APPENDIX B. APPENDIX B

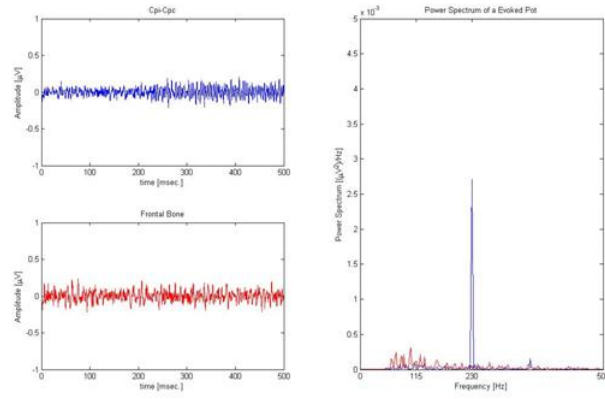


Figure B.1

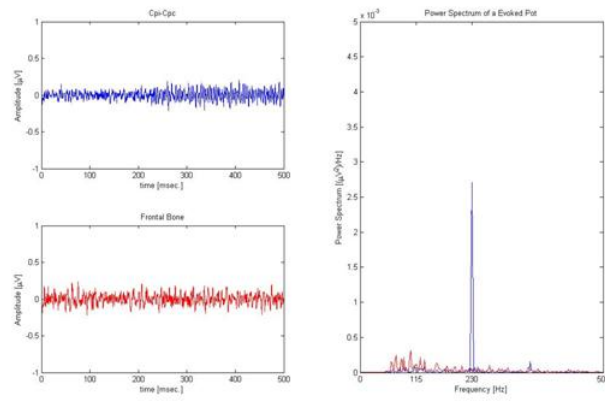


Figure B.2

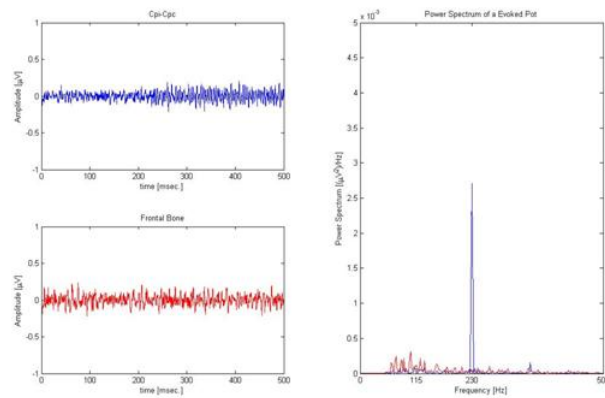


Figure B.3

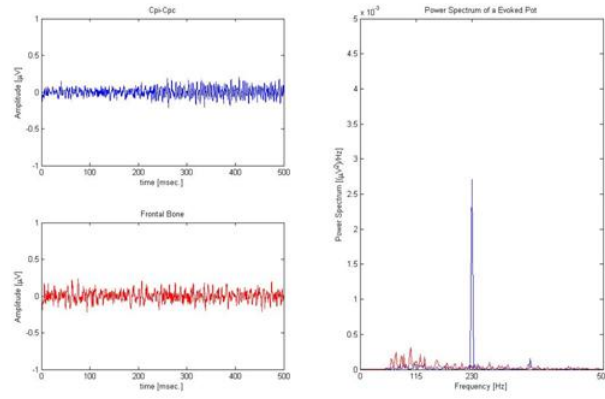


Figure B.4

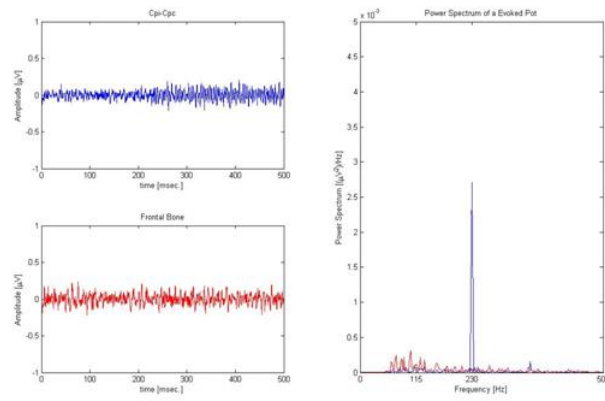


Figure B.5

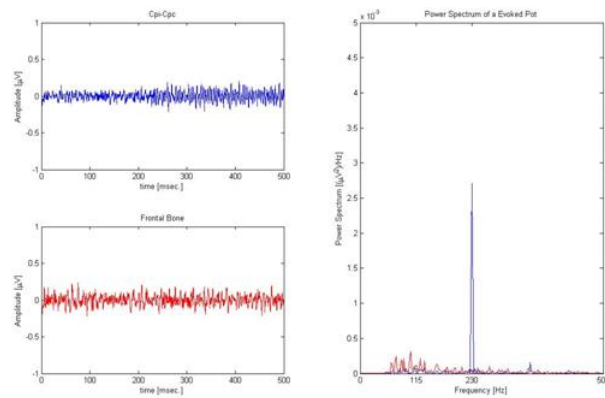


Figure B.6

APPENDIX C. APPENDIX C

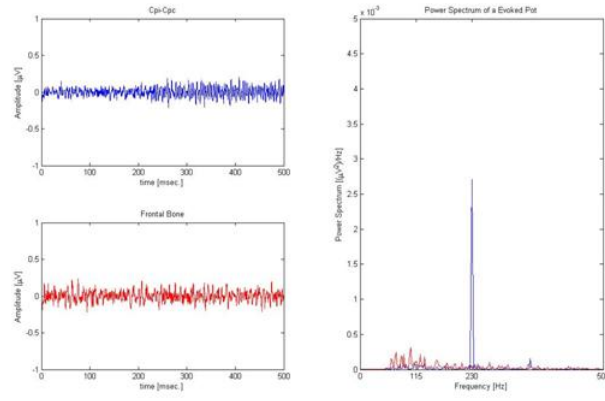


Figure C.1

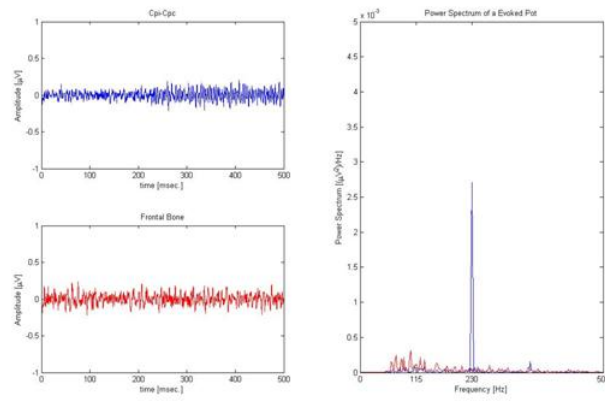


Figure C.2

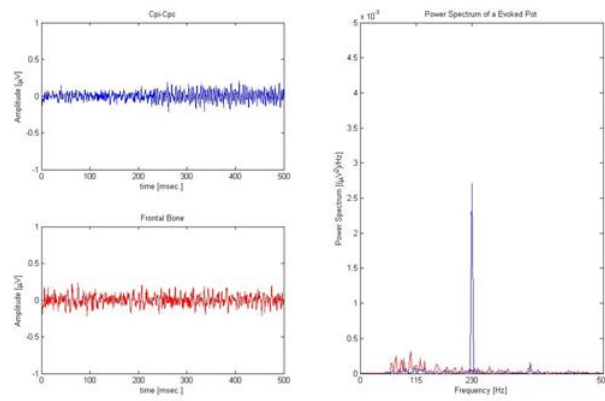


Figure C.3

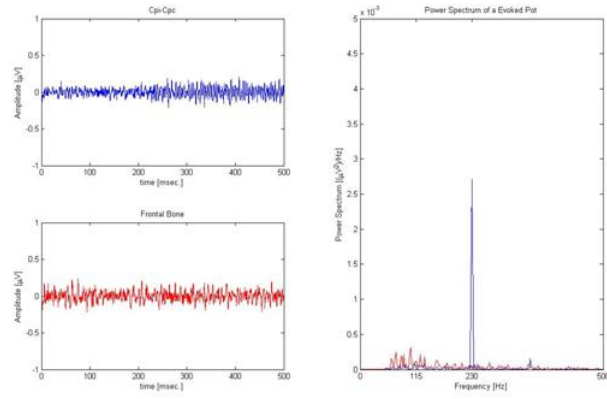


Figure C.4

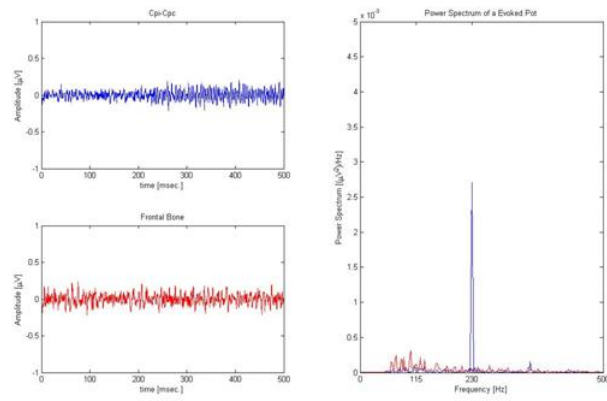


Figure C.5

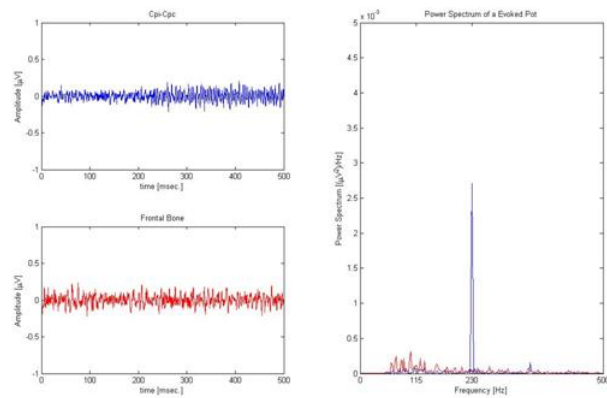


Figure C.6

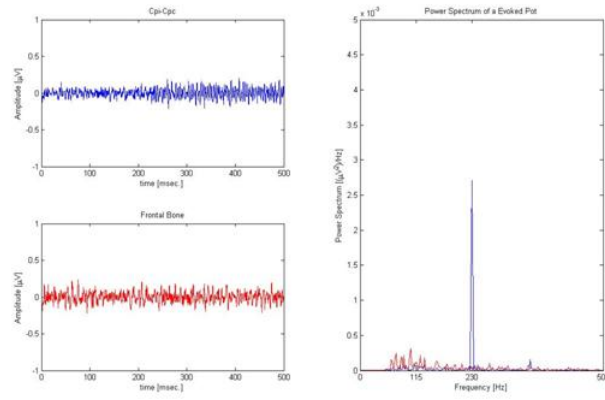


Figure C.7

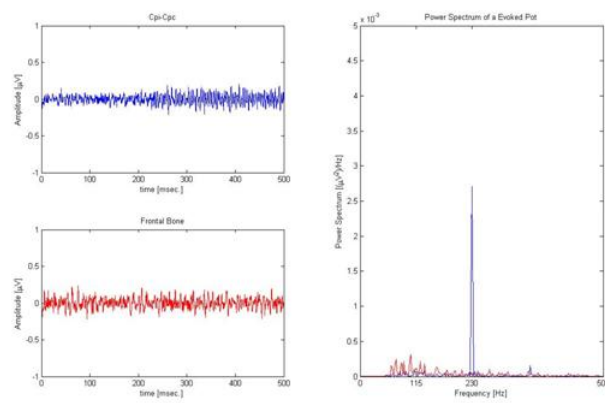


Figure C.8

REFERENCES

1. M.F. Bear, B.W. Connor, M. P., *Neuroscience: Exploring the Brain, 2nd ed.*, Philadelphia, Pennsylvania, USA: Lippincot Williams & Wilkins Press, 2001.
2. Greenspan, J. D., and S. J. Bolanowski, "The psychophysics of tactile perception and its peripheral physiological basis," *Pain and Touch*, 1996.
3. B., and S. J. Bolanowski, "Vibrotactile thresholds of the non-pacinian i channel: I.methodological issues," *Somatosensory and Motor Research*, Vol. 22, no. 1/2, pp. 49–56, 2005.
4. nal, B., "Tactile sensitivity of normal and autistic children," *Somatosensory and Motor Research*, Vol. 24, no. 1, pp. 21–23, 2007.
5. G.A. Geschieder, A. G., *Psychophysics : The Fundamentals, 3rd ed.*, London, UK: Lawrance Erlbaum Associates Inc., 1997.
6. Bolanowski, S. J., G. Geschieder, V. T. Verrillo, and C. M. Checkosky, "Four channels mediate the mechanical aspects of touch," *J. Acoust. Soc. Am.*, Vol. 84, pp. 1680–1694, 1988.
7. Bolanowski, S. J., G. Geschieder, and K. Hardick, "The frequency selectivity of information-processing channels in the tactile sensory system," *Somatosensory and Motor Research*, Vol. 18, pp. 191–201, 2001.
8. Gescheider, G., S. Bolanowski, and R. Verillo, "Some characteristics of tactile channels," *Behavioural Brain Research*, Vol. 148, pp. 35–40, 2004.
9. Subcommittee, A. S. E. P., "Somatosensory evoked potentials:clinical usage," *Muscle Nerve*, Vol. 85, pp. 225–238, Jan 1996.
10. K.E. Misulis, T., *Spehlmann's Evoked Potential Primer, 3rd Edition*, Oxford: Butterworth-Heinemann, 2001.
11. M.J.Aminoff, and A. A., "Aaem minimonograph 19: Somatosensory evoked potentials," *Muscle and Nerve*, Vol. 21, pp. 277–290, 1998.
12. S.J.Bolanowski, "Somatosensory coding; signals and perception, the human fundamentals of sensation," *Open University Course, Milton Keynes*, Vol. 18, pp. 233–243, 2005.
13. Bensmaia, S., J. Craig, T. Yoshioka, and K. Johnson, "Sai and ra afferent responses to static and vibrating gratings," *Journal of Neurophysiology*, Vol. 95, pp. 1771–1782, 2006.
14. Güçlü, B., and S. J. Bolanowski, "Distribution of the intensity-characteristic parameters of cat rapidly adapting mechanoreceptive fibers," *Somatosensory Motor Research*, Vol. 20, pp. 149–155, 2003a.
15. E. R. Kandel, J. H. Schwartz, T. M. J., *Principle of Neuroscience, 4th Edition*, USA: McGraw Hill, 2000.
16. Güçlü, B., and S. J. Bolanowski, "Frequency responses of cat rapidly adapting mechanoreceptive fibers," *Somatosensory Motor Research*, Vol. 20, no. 3, pp. 249–263, 2003.

17. Güçlü, B., and S. J. Bolanowski, "Tristate markov model for the firing statistics of rapidly-adapting mechanoreceptive fibers," *Journal of Computational Neuroscience*, Vol. 17, pp. 107–126, 2004a.
18. Güçlü, B., and S. J. Bolanowski, "Modeling population responses of rapidly-adapting mechanoreceptive fibers," *Journal of Computational Neuroscience*, Vol. 12, pp. 201–218, 2002.
19. Güçlü, B., and S. J. Bolanowski, "Probability of stimulus detection in a model population of rapidly adapting fibers," *Neural Comput.*, Vol. 16, pp. 39–58, 2004b.
20. F. E. Kelly, S. E. F., "Eeg evidence of stimulus-directed response dynamics in human somatosensory cortex," *Brain Research*, Vol. 815, pp. 326–336, 1996.
21. F. E. Kelly, M. Trulsson, S. E. F., "Periodic microstimulation of single mechanoreceptive afferents produces frequency-following responses in human eeg," *Journal of Neurophysiology*, Vol. 77, pp. 137–144, 1997.
22. Unser, M., and A. Aldroubi, "Review of the wavelets in biomedical applications," *Proceeding of the IEEE*, Vol. 84, pp. 626–638, 1996.
23. F., N. C., and L. Lai, "Wavelet-based algorithm for signal analysis," *EURASIP Journal on Advances in Signal Processing*, Vol. 10, 2007.
24. A. Mouraux, G. I., "Across-trial averaging of event-related eeg responses and beyond," *Magnetic Resonance Imaging*, Vol. 0, pp. 730–725, 2008.
25. Addison, P., *The Illustrated Wavelet Transform Handbook : Introductory Theory and Applications in Science, Engineering, Medicine and Finance*, England, UK: Institute of Physics Publishing Bristol and Philadelphia, 2000.